

## Intrinsic Vibrational Angular Momentum from Nonadiabatic Effects in Noncollinear Magnetic Molecules

Oliviero Bistoni,<sup>1,2</sup> Francesco Mauri<sup>3</sup>, and Matteo Calandra<sup>1,2,\*</sup>

<sup>1</sup>*Sorbonne Université, CNRS, Institut des Nanosciences de Paris, UMR 7588, F-75252 Paris, France*

<sup>2</sup>*Dipartimento di Fisica, Università di Trento, Via Sommarive 14, 38123 Povo, Italy*

<sup>3</sup>*Dipartimento di Fisica, Università di Roma La Sapienza, Piazzale A. Moro 5, I-00185 Roma, Italy*



(Received 16 November 2020; revised 12 February 2021; accepted 21 April 2021; published 4 June 2021)

We show that in noncollinear magnetic molecules, nonadiabatic (dynamical) effects due to the electron-vibron coupling are time-reversal symmetry breaking interactions for the vibrational field. Because the electronic wave function cannot be chosen as real in these molecules, a nonzero geometric vector potential (Berry connection) arises. As a result, an intrinsic nonzero vibrational angular momentum occurs even for nondegenerate modes and in the absence of external probes. The vibronic modes can then be seen as elementary quantum particles carrying a sizeable angular momentum. As a proof of concept, we demonstrate the magnitude of this topological effect by performing nonadiabatic first principles calculations on platinum clusters and by showing that these molecules host sizeable intrinsic phonon angular momenta comparable to the orbital electronic ones in itinerant ferromagnets.

DOI: [10.1103/PhysRevLett.126.225703](https://doi.org/10.1103/PhysRevLett.126.225703)

Several experiments have demonstrated the non-negligible interaction between vibrational modes and magnetic fields or optical probes. The phonon Hall effect [1–3] and the phonon contribution to the gyromagnetic ratio detected in the Einstein–de Haas effect [4,5] are eminent examples. Moreover, it has been demonstrated that valley selective infrared optical absorption in transition metal dichalcogenides breaks time-reversal symmetry for the phonon field and can be used to probe the chirality of phonon modes at particular points in the Brillouin zone [6,7].

In the absence of external probes, phonons are usually understood in terms of springs and as such they are considered as linearly polarized, so they do not break time-reversal symmetry and they are not supposed to carry a finite angular momentum. An intrinsic phonon angular momentum can be obtained from a twofold degenerate vibrational mode, as a linear combination of two linear phonon eigenvectors can lead to a circularly polarized mode in the same way as circularly polarized light can arise from two linear polarizations. This case has been investigated in the literature extensively [7–11], particularly for hexagonal crystal lattices [12]. For each circularly polarized phonon carrying an angular momentum  $\mathcal{L}$ , there exists another linearly independent combination of linear polarizations leading to an angular momentum  $-\mathcal{L}$ , so that the total phonon angular momentum for the degenerate modes is zero. An external time-reversal symmetry breaking probe, such as optical absorption or an external magnetic field, is then needed to break the degeneracy.

The question of whether a nondegenerate phonon mode can host an intrinsic angular momentum without external probes is still open. Specifically, can an intrinsic

mechanism lead to a time-reversal symmetry breaking in the phonon field?

In this Letter, we demonstrate that nonadiabatic (dynamical) effects due to the electron-vibron interaction generate synthetic gauge fields in insulating noncollinear magnetic molecules. We provide the microscopic link between topology and the electron-vibron interaction by showing that in these molecules a nonzero Berry curvature leads to a finite intrinsic vibrational angular momentum even for nondegenerate modes and in the absence of external magnetic fields. As a proof of concept, we demonstrate the effect by performing nonadiabatic first principles calculations on platinum clusters.

We introduce a cumulative index  $\lambda = (I, \alpha)$  for the Cartesian coordinates  $\alpha = x, y, z$  of the  $I$ th atom in a molecule. The atomic position in a molecule is  $R_\lambda = R_\lambda^{\text{eq}} + u_\lambda$ , where  $R_\lambda^{\text{eq}}$  are the coordinates of the atomic equilibrium positions and  $u_\lambda$  is the Cartesian component of the ionic displacement of the  $I$ th atom. In the Born-Oppenheimer approximation, the quantum-mechanical Hamiltonian for the ionic motion reads [13]

$$\mathcal{H} = \frac{1}{2M} \sum_\lambda [p_\lambda - \hbar \mathcal{A}_\lambda(\mathbf{u})]^2 + E(\mathbf{u}), \quad (1)$$

where  $p_\lambda = -i\hbar \nabla_{u_\lambda} \equiv -i\hbar \nabla_\lambda$  is the ionic momentum,  $\mathcal{A}_\lambda(\mathbf{u}) = i \langle \Psi(\mathbf{u}) | \nabla_\lambda \Psi(\mathbf{u}) \rangle$  is a geometric vector potential (the so-called Berry potential or Berry connection),  $E(\mathbf{u})$  is the potential energy felt by the ions due to the electrons, and  $|\Psi(\mathbf{u})\rangle$  is the ground-state electronic wave function that depends parametrically on the nuclear displacements  $\mathbf{u}$ . For

ease of notation, we consider equal masses for all the atoms, as this also corresponds to the case treated in this Letter.

In the absence of external magnetic fields and noncollinear magnetic order, the electronic wave function  $|\Psi(\mathbf{u})\rangle$  can be taken as real, and the geometric vector potential in Eq. (1) is zero [14]. On the other hand, in the absence of an external magnetic field but for a noncollinear magnetic molecule, the electronic wave function is complex and cannot be chosen as real, so that  $\mathcal{A}_\lambda(\mathbf{u})$  is nonzero and nontrivial geometric effects may occur.

The Berry curvature is defined as  $\Omega_{\lambda\eta} = \partial_\lambda \mathcal{A}_\eta - \partial_\eta \mathcal{A}_\lambda$ , where  $\partial_\lambda \equiv \partial/\partial u_\lambda$ . In linear response theory,  $\Omega_{\lambda\eta}$  does not depend on the parameter  $\mathbf{u}$  as the derivatives are evaluated at  $\mathbf{u} = 0$ . In the Heisenberg representation, the equation of motion for the nuclear displacement reads [15]

$$M\ddot{u}_\lambda + \hbar \sum_\eta \Omega_{\lambda\eta} \dot{u}_\eta + \partial_\lambda E = 0. \quad (2)$$

In the harmonic approximation, we expand the potential energy up to the second order in the ionic displacement. Using monochromatic solutions in  $\omega$ , the equation of motion can thus be written as

$$\frac{1}{M} \sum_\eta [C_{\lambda\eta} - i\hbar\omega\Omega_{\lambda\eta}] e_\eta = \omega^2 e_\lambda, \quad (3)$$

where  $C_{\lambda\eta} = \partial_\lambda \partial_\eta E$  is the static harmonic force-constant matrix, and  $e_\lambda$  are the vibrational polarization vectors. The term in  $\Omega_{\lambda\eta}$  is an effective Lorentz force exerted by the geometrical magnetic field (note that  $\Omega_{\lambda\eta}$  is a real antisymmetric matrix). The formal solution of the nonlinear eigenvalue equation (3), can be found in the supplemental material of Ref. [5].

At zero temperature, the expectation value of the quantum vibrational angular momentum  $\mathbf{L} = \sum_I \mathbf{u}_I \times \dot{\mathbf{u}}_I$  over the quantum vibron ground state reads [5]  $\langle \mathbf{L} \rangle = \sum_\nu \boldsymbol{\ell}_\nu$ , where  $\nu$  labels the vibrational modes and  $\boldsymbol{\ell}_\nu$  can be expressed in terms of (the Cartesian components of) the vibrational polarization vectors  $\mathbf{e}_{I\nu}$  as

$$\boldsymbol{\ell}_\nu = -i\hbar \sum_I \mathbf{e}_{I\nu}^* \times \mathbf{e}_{I\nu}. \quad (4)$$

We underline that the expectation value of the cartesian components of  $\mathbf{L}$  over the vibron ground state, i.e.,  $\langle L_\alpha \rangle = \sum_\nu \ell_{\nu,\alpha}$ , where  $\alpha = x, y, z$ , is not a quantized object and can assume any value. Indeed, while in the absence of noncollinear magnetism and in the presence of an external magnetic field along the  $z$  direction,  $L_z$  commutes with  $\mathcal{H}$  in Eq. (1), in the case of noncollinear magnetism treated here, the components of the phonon angular momentum  $L_\alpha$  do not commute with  $\mathcal{H}$ . Thus, in

our case, the ground state of Eq. (1) is not an eigenstate of  $L_\alpha$  and neither  $\sum_\nu \ell_{\nu,\alpha}$  nor  $\ell_{\nu,\alpha}$  are quantized.

If the Berry curvature  $\Omega_{\lambda\eta}$  in Eq. (3) vanishes (i.e., for real wave functions), the polarization vectors are eigenfunctions of the static and real force constant matrix  $C_{\lambda\eta}$  and therefore they themselves are real (up to an irrelevant global phase factor) and the angular momentum  $\boldsymbol{\ell}_\nu$  is equal to zero (since  $\mathbf{e}^* = \mathbf{e}$ ). On the contrary, in molecules with noncollinear magnetism, the electronic wave functions are necessarily complex and the Berry curvature does not vanish. The polarization vectors of Eq. (3) are therefore intrinsically complex and give rise to a nonzero vibrational angular momentum. Thus, the occurrence of a vibrational mode with a finite angular momentum is intimately connected with the existence of a geometrical or physical gauge field.

We now show that, in the independent electron approximation, both Eq. (3) and the existence of a nonzero intrinsic angular momentum for a molecular vibrational mode naturally arise from the theory of nonadiabatic (dynamical) effects developed in Ref. [16], providing the link between the electron-vibron interaction, topological effects, and the existence of a nonzero intrinsic vibrational angular momentum. Within time dependent density functional theory and in the adiabatic local density approximation, the dynamical force constant matrix for frequencies  $\omega$  smaller than the HOMO-LUMO gap ( $\Delta$ ) reads

$$C_{\lambda\eta}(\omega) = C_{\lambda\eta} + \Pi_{\lambda\eta}(\omega), \quad (5)$$

where  $C_{\lambda\eta}$  is the static force constant matrix and  $\Pi_{\lambda\eta}(\omega)$  can be written in perturbation theory as

$$\begin{aligned} \Pi_{\lambda\eta}(\omega) = 2 \sum_{m,n} \left[ \frac{f_m - f_n}{\epsilon_m - \epsilon_n + \hbar\omega} - \frac{f_m - f_n}{\epsilon_m - \epsilon_n} \right] \\ \times \langle \psi_n | \partial_\lambda H_{\text{KS}} | \psi_m \rangle \langle \psi_m | \partial_\eta H_{\text{KS}} | \psi_n \rangle. \end{aligned} \quad (6)$$

Here  $|\psi_m\rangle$ ,  $\epsilon_m$ , and  $f_m$  are the Kohn-Sham wave functions, energy levels, and Fermi occupations at equilibrium positions (i.e.,  $\mathbf{u} = 0$ ), respectively, and  $H_{\text{KS}}$  is the electronic Kohn-Sham Hamiltonian. The deformation potential matrix element  $\langle \psi_m | \partial_\eta H_{\text{KS}} | \psi_n \rangle$  is related to the electron-vibron interaction. The nonadiabatic (dynamical) vibrational frequencies ( $\tilde{\omega}_\nu$ ) and polarization vectors ( $\tilde{\mathbf{e}}_{\eta\nu}$ ), which will be marked hereinafter with a tilde, are obtained from the nonlinear eigenvalue equation

$$\frac{1}{M} \sum_\eta C_{\lambda\eta}(\tilde{\omega}_\nu) \tilde{\mathbf{e}}_{\eta\nu} = \tilde{\omega}_\nu^2 \tilde{\mathbf{e}}_{\lambda\nu}. \quad (7)$$

When  $\hbar\omega \ll \Delta$ , Eq. (5) can be expanded at first order to obtain

$$C_{\lambda\eta}(\omega) = C_{\lambda\eta} - i\hbar\omega\Omega_{\lambda\eta}^{\text{KS}} + \mathcal{O}(\omega^2), \quad (8)$$

where  $\Omega_{\lambda\eta}^{\text{KS}} = \sum_m f_m \Omega_{\lambda\eta,m}^{\text{KS}}$  and  $\Omega_{\lambda\eta,m}^{\text{KS}}$  is the Berry curvature of the  $m$ th Kohn-Sham state [14] with respect to the atomic displacement, namely

$$\Omega_{\lambda\eta,m}^{\text{KS}} = -2\text{Im} \sum_{n \neq m} \frac{1}{(\epsilon_m - \epsilon_n)^2} \times \langle \psi_m | \partial_\lambda H_{\text{KS}} | \psi_n \rangle \langle \psi_n | \partial_\eta H_{\text{KS}} | \psi_m \rangle. \quad (9)$$

The matrix  $\Omega_{\lambda\eta}^{\text{KS}}$  is a real antisymmetric matrix that plays the role of  $\Omega_{\lambda\eta}$  in the case of Kohn-Sham independent electrons. The nonadiabatic (dynamical) vibrational frequencies  $\tilde{\omega}_\nu$  and polarization vectors  $\tilde{e}_{I\nu}$  can then be obtained as solutions of the nonlinear eigenvalue equation (7), and used to calculate the quantum angular momentum via Eq. (4).

Equations (8) and (9) are the microscopic link between the electron-vibron interaction, nonadiabatic (dynamical) effects, and the occurrence of a finite angular momentum in molecules. Furthermore, they provide a practical computational scheme of the vibrational quantum angular momentum using the theory proposed in Ref. [16]. Since  $\Omega_{\lambda\eta}$  is proportional to the square of the deformation potential and inversely proportional to the HOMO-LUMO gap, Eq. (9) suggests that large nonadiabatic (dynamical) effects and vibrational angular momenta could be found in noncollinear magnetic molecules with a small gap and a large electron-vibron interaction.

We demonstrate the occurrence of an intrinsic total vibrational angular momentum due to nonadiabatic (dynamical) effects by considering platinum clusters, namely a trimer  $\text{Pt}_3$  and a pentamer  $\text{Pt}_5$ . These systems are ideal as (i) they are magnetic, (ii) the large spin-orbit coupling leads to noncollinear magnetic structures, and (iii) the HOMO-LUMO gap is very small.

We calculate the electronic structure and the vibrational properties (adiabatic and nonadiabatic) of  $\text{Pt}_3$  and  $\text{Pt}_5$  by performing fully relativistic calculations using version 6.4.1 of the QUANTUM-ESPRESSO suite [17] and the compatible version of THERMO\_PW[18] for the noncollinear treatment of the magnetization densities. We used version 3.3.0 of the fully relativistic ONCV pseudopotential [19,20] with the Perdew-Burke-Ernzerhof exchange-correlation functional [21] and a kinetic energy cutoff of 120 Ry. A simple cubic Bravais lattice structure with a parameter of 10.6 Å was used in order to minimize the interaction between the molecules and their copies. The binding energy per atom of each cluster is obtained as  $(nE_1 - E_n)/n$ , where  $n$  is the number of atoms in the cluster and  $E_1$  is the energy of the isolated atom.

We find that the lowest-energy structure of  $\text{Pt}_3$  is an isosceles triangle with interatomic distances of 2.489 Å and 2.501 Å, as shown in Fig. 1. The binding energy per atom is 2.177 eV. The HOMO-LUMO gap is  $\Delta = 137$  meV in agreement with [22,23]. The total magnetization is 1.58  $\mu_B$ .

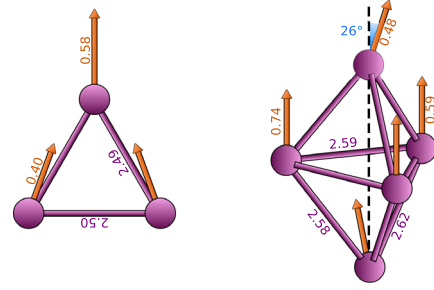


FIG. 1. Noncollinear magnetic ground state of  $\text{Pt}_3$  and  $\text{Pt}_5$  structure, interatomic distances, and magnetic momenta.

For  $\text{Pt}_5$ , we obtain as the lowest energy structure a noncollinear magnetic trigonal bipyramid with the vertex atoms slightly shifted toward one side of the basis triangle. The interatomic distances and the noncollinear magnetic atomic momenta are shown in Fig. 1. The calculated binding energy per atom is 2.835 eV in agreement with [24]. The HOMO-LUMO gap is  $\Delta = 92$  meV, and the total magnetization is 3.63  $\mu_B$  in agreement with [23]. The smallness of  $\Delta$  suggests the occurrence of large nonadiabatic effects in  $\text{Pt}_3$  and  $\text{Pt}_5$ .

Once the magnetic ground state is converged, we study the vibrational properties of the Pt clusters using linear response theory. The adiabatic (static) optical frequencies of  $\text{Pt}_3$  and  $\text{Pt}_5$  are shown in the second column of Table I.

Then the nonlinear eigenvalue equation (7), is solved by simply evaluating the force-constant matrix  $C_{\lambda\eta}(\omega)$  at different frequencies and by diagonalizing it. For each mode, the nonadiabatic (dynamical) vibrational frequency and polarization vectors can be found when the square root of the eigenvalue is equal to the value of the frequency input into the dynamical force constant matrix. The optical frequencies thus obtained are shown in the fourth column of Table I for  $\text{Pt}_3$  and  $\text{Pt}_5$ . We find that in  $\text{Pt}_3$  and  $\text{Pt}_5$ , the nonadiabatic effects are small and do not modify the frequency of the optical modes substantially. The vibrational frequencies  $\tilde{\omega}'_\nu$  obtained by solving the nonlinear eigenvalue equation (7), having replaced  $C_{\lambda\eta}(\tilde{\omega}_\nu)$  with the low-energy expansion of the dynamical matrix, Eq. (8), are shown in column 5 of Table I.

Nonadiabatic (dynamical) effects modify the oscillatory motion of the ions around their equilibrium positions. The phonon ionic displacements are related to the polarization vectors through  $\mathbf{u}_I = \text{Re}[\tilde{e}_{I\nu} e^{-i\tilde{\omega}'_\nu t}]$ . In the adiabatic case, the polarization vectors  $\mathbf{e}_{I\nu}$  are real, and the ionic motion reduces to a one-dimensional oscillation. Instead, in the nonadiabatic case, the polarization vectors  $\tilde{e}_{I\nu}$  are complex, and therefore the ions perform elliptical trajectories around their equilibrium positions. Consequently, each ion gives rise to an orbital angular momentum perpendicular to the plane of the orbit. For each mode, the angular momentum of the molecule is equal to the sum of the angular momenta of the rotating ions. It can be evaluated by replacing the nonadiabatic phonon polarization vectors  $\tilde{e}_{I\nu}$  into Eq. (4).

TABLE I. Nonadiabatic effects in the optical modes of Pt<sub>3</sub> and Pt<sub>5</sub>. From left to right, adiabatic mode index  $\nu$ ; adiabatic vibrational frequencies  $\omega_\nu$ ; nonadiabatic frequencies  $\tilde{\omega}_\nu$ ; nonadiabatic frequencies  $\tilde{\omega}'_\nu$  obtained from the low-energy expansion of the dynamical matrix, Eq. (8); Cartesian components of the angular momentum  $\ell_\nu$  in units of  $\hbar/2$ .

	$\nu$	$\omega_\nu$ (cm <sup>-1</sup> )	$\tilde{\omega}_\nu$ (cm <sup>-1</sup> )	$\tilde{\omega}'_\nu$ (cm <sup>-1</sup> )	$\ell_{\nu x}$ ( $\hbar/2$ )	$\ell_{\nu y}$ ( $\hbar/2$ )	$\ell_{\nu z}$ ( $\hbar/2$ )
Pt <sub>3</sub>	1	102.4	100.6	102.5	-0.048	0.000	0.000
	2	121.7	121.2	121.7	0.000	0.000	0.000
	3	217.7	217.7	217.7	0.001	0.000	0.000
Pt <sub>5</sub>	1	54.0	53.6	54.0	0.000	0.000	-0.064
	2	71.1	71.1	71.1	0.000	0.000	-0.094
	3	97.0	96.6	96.7	0.001	0.000	-0.089
	4	103.3	103.5	103.5	0.002	0.000	-0.086
	5	119.6	119.5	119.6	0.002	0.000	0.000
	6	134.8	134.7	134.7	-0.003	0.000	0.071
	7	138.6	138.6	138.6	0.000	0.000	0.093
	8	169.4	169.4	169.5	0.000	0.000	0.001
	9	210.4	209.9	210.5	0.000	0.000	-0.003

As an illustrative example, we represent in Fig. 2 the adiabatic and nonadiabatic polarization vectors of two stretching modes of Pt<sub>3</sub> and Pt<sub>5</sub>. In both cases, the polarization vectors acquire an imaginary part and the nonadiabatic mode carries nonzero angular momentum.

The angular momentum of the optical modes of Pt<sub>3</sub> and Pt<sub>5</sub> is listed in the right-hand side of Table I. Unexpectedly, we record a sizeable vibrational angular momentum even where the vibrational frequency is marginally altered by the

nonadiabatic (dynamical) effects. The magnitude of these vibrational angular momenta is of the same order of the typical values of the electron orbital momenta in itinerant ferromagnets [25].

The total phonon angular momentum  $\langle \mathbf{L} \rangle = \sum_\nu \ell_\nu$  is nonzero because the angular momentum  $\ell_\nu$  is calculated at a different frequency for each mode  $\nu$ . Since the angular momentum of the molecule must be conserved, a non-adiabatic variation of the electron angular momentum (spin plus orbital) must also occur in order to compensate the phonon contribution. The calculation of such variation, however, requires simulating the nonadiabatic dynamics of the whole molecule, which goes beyond the purpose of this work.

In conclusion, we have shown that in noncollinear magnetic molecules, nonadiabatic (dynamical) effects due to the electron-vibron coupling are time-reversal symmetry breaking interactions for the vibrational field. Because the electronic wave function cannot be chosen as real in these molecules, a nonzero geometric vector potential arises. As a result, an intrinsic nonzero phonon angular momentum occurs even for nondegenerate modes and in the absence of external time-reversal symmetry breaking probes. Our work provides the conceptual link between topology, electron-phonon interaction, and the existence of a nonzero intrinsic phonon angular momentum in insulating noncollinear magnetic molecules.

As a proof of concept, we have demonstrated the magnitude of this topological effect by performing non-adiabatic first principles calculations on platinum clusters and by showing that vibrons host sizeable intrinsic angular momenta with a magnitude comparable to the typical orbital electronic angular momenta in itinerant ferromagnets [25]. As the same conclusions obtained for a molecule can be easily generalized to an insulating crystal, we expect that in any noncollinear magnetic system (solid or molecule) with strong electron-phonon interaction and a

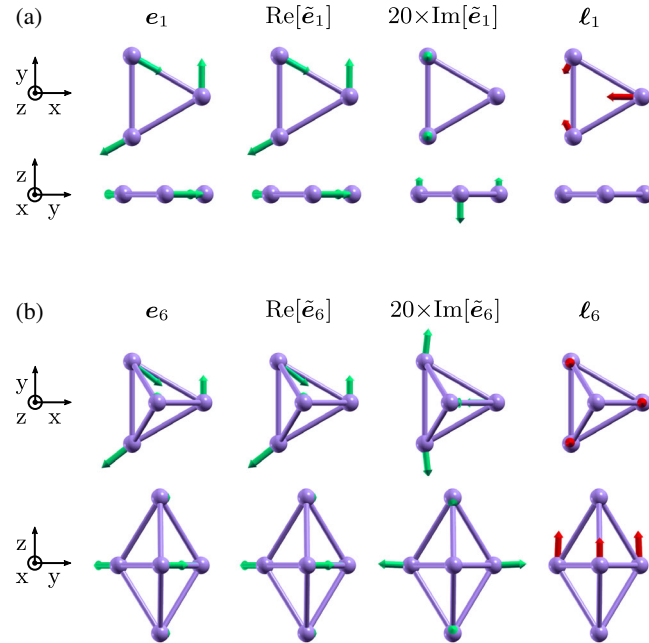


FIG. 2. From left to right, top (x-y) and side (y-z) representation of the adiabatic (static) polarization vectors  $e_\nu$ , of the real and imaginary parts of the nonadiabatic (dynamical) polarization vectors  $\tilde{e}_\nu$  and of the vibrational angular momentum  $\ell_\nu$ . (a) Asymmetric stretching mode of Pt<sub>3</sub> ( $\nu = 1$ ). (b) Asymmetric stretching mode of Pt<sub>5</sub> ( $\nu = 6$ ).

sufficiently small gap, the nonadiabatic effects break time-reversal symmetry and generate sizeable intrinsic phonon angular momenta.

Finally, a question arises as to whether the angular momenta of phonons can be observable in experiments. There are two cases in which it can be detected. The first is the case in which a twofold degenerate mode at zone center occurs in the adiabatic phonon frequencies of the non-collinear magnetic system. As the time-reversal symmetry breaking nonadiabatic term related to the Berry connection in Eqs. (1) and (3) lowers the crystal symmetry, then the twofold degenerate mode could split in two different modes hosting different angular momenta. In this case, even if the angular momentum itself was not observed, its effects on the phonon spectrum would be. The second case is infrared absorption from left and right circularly polarized modes. As the vibrational angular momentum affects the atomic dipoles, the infrared intensities could be different for different circular polarizations.

We acknowledge IDRIS, CINES, TGCC, PRACE, and CINECA for high performance computing resources. We acknowledge P. Giannozzi and J. Carusotto for useful discussions.

---

\*Corresponding author.

m.calandrabuonaura@unitn.it

- [1] C. Strohm, G. L. J. A. Rikken, and P. Wyder, *Phys. Rev. Lett.* **95**, 155901 (2005).
- [2] A. V. Inyushkin and A. N. Taldenkov, *JETP Lett.* **86**, 379 (2007).
- [3] L. Zhang, *New J. Phys.* **18**, 103039 (2016).
- [4] A. Einstein and W. J. de Haas, *Verh. Dtsch. Phys. Ges.* **17**, 152 (1915); **18**, 696 (1915).
- [5] L. Zhang and Q. Niu, *Phys. Rev. Lett.* **112**, 085503 (2014).
- [6] H. Zhu, J. Yi, M.-Y. Li, J. Xiao, L. Zhang, C.-W. Yang, R. A. Kaindl, L.-J. Li, Y. Wang, and X. Zhang, *Science* **359**, 579 (2018).
- [7] L. Zhang and Q. Niu, *Phys. Rev. Lett.* **115**, 115502 (2015).
- [8] Y. Liu, C.-S. Lian, Y. Li, Y. Xu, and W. Duan, *Phys. Rev. Lett.* **119**, 255901 (2017).
- [9] X. Xu, W. Zhang, J. Wang, and L. Zhang, *J. Phys. Condens. Matter* **30**, 225401 (2018).
- [10] X. Xu, H. Chen, and L. Zhang, *Phys. Rev. B* **98**, 134304 (2018).
- [11] H. Chen, W. Wu, S. A. Yang, X. Li, and L. Zhang, *Phys. Rev. B* **100**, 094303 (2019).
- [12] In hexagonal crystal lattices with broken in-plane inversion symmetry (e.g., BN monolayer), single degenerate phonon modes carry opposite angular momenta at the Brillouin zone corners  $\mathbf{K}$  and  $\mathbf{K}' = -\mathbf{K}$ . However, the phonon modes at  $\mathbf{K}$  and  $\mathbf{K}'$  have the same energy, and if vibrations are described in a  $\sqrt{3} \times \sqrt{3}R30^\circ$  supercell,  $\mathbf{K}$  and  $\mathbf{K}'$  fold into  $\Gamma$  and the two single degenerate modes become twofold degenerate at zone center.
- [13] T. Qin, J. Zhou, and J. Shi, *Phys. Rev. B* **86**, 104305 (2012).
- [14] R. Resta, *J. Phys. Condens. Matter* **12**, R107 (2000).
- [15] T. Saito, K. Misaki, H. Ishizuka, and N. Nagaosa, *Phys. Rev. Lett.* **123**, 255901 (2019).
- [16] M. Calandra, G. Profeta, and F. Mauri, *Phys. Rev. B* **82**, 165111 (2010).
- [17] P. Giannozzi, S. Baroni, N. Bonini, M. Calandra, R. Car, C. Cavazzoni, D. Ceresoli, G. L. Chiarotti, M. Cococcioni, I. Dabo *et al.*, *J. Phys. Condens. Matter* **21**, 395502 (2009); P. Giannozzi, O. Andreussi, T. Brumme, O. Bunau, M. B. Nardelli, M. Calandra, R. Car, C. Cavazzoni, D. Ceresoli, M. Cococcioni *et al.*, *J. Phys. Condens. Matter* **29**, 465901 (2017).
- [18] A. Urru and A. Dal Corso, *Phys. Rev. B* **100**, 045115 (2019).
- [19] D. R. Hamann, *Phys. Rev. B* **88**, 085117 (2013).
- [20] M. van Setten, M. Giantomassi, E. Bousquet, M. Verstraete, D. Hamann, X. Gonze, and G.-M. Rignanese, *Comput. Phys. Commun.* **226**, 39 (2018).
- [21] J. P. Perdew, K. Burke, and M. Ernzerhof, *Phys. Rev. Lett.* **77**, 3865 (1996).
- [22] M. N. Huda, M. K. Niranjana, B. R. Sahu, and L. Kleinman, *Phys. Rev. A* **73**, 053201 (2006).
- [23] H. Yuan, H. Chen, A. Kuang, and B. Wu, *J. Magn. Magn. Mater.* **331**, 7 (2013).
- [24] P. Błoński, S. Dennler, and J. Hafner, *J. Chem. Phys.* **134**, 034107 (2011).
- [25] D. Ceresoli, U. Gerstmann, A. P. Seitsonen, and F. Mauri, *Phys. Rev. B* **81**, 060409(R) (2010).